

AN UNVEILING EVENT IN THE TYPE 2 AGN NGC4388: A CHALLENGE FOR A PARSEC SCALE ABSORBER

MARTIN ELVIS¹, G. RISALITI^{1,2}, F. NICASTRO¹, J. M. MILLER^{1,3}, F. FIORE⁴, AND S. PUC CETTI⁴

Draft version December 24, 2018

ABSTRACT

We present two *Rossi X-ray Timing Explorer* (RXTE) PCA observations of the type 2 Seyfert galaxy NGC 4388 caught in an unusual low X-ray absorption state. The observations were triggered by a detection in the 1.5-3 keV band of the RXTE All-Sky Monitor. NGC 4388 was found at a somewhat high continuum level ($f(2-10\text{ keV})=8\times 10^{-11}\text{ erg cm}^{-2}\text{ s}^{-1}$) and with a column density ($N_H\sim 3\times 10^{22}\text{ cm}^{-2}$), a factor ~ 10 lower than normal. The second PCA observation, four hours later, gave $N_H < 2\times 10^{21}\text{ cm}^{-2}$ indicating, at the 3.1σ level, variability so rapid puts the absorber on a few 100 Schwarzschild radii scale, similar to the Broad Emission Line Region, or smaller. This small scale creates difficulties for the parsec-scale obscuring torus paradigm of Unified Schemes for type 1 and type 2 AGNs.

Subject headings:

1. INTRODUCTION

Optically NGC 4388 is a classical type 2 Seyfert galaxy (Huchra, Wyatt & Davis 1982) with permitted and forbidden emission lines of the same width (Khachikian & Weedman 1974). There is abundant evidence that many, and perhaps all, type 2 Active Galactic Nuclei (AGNs) are normal type 1 AGNs with both the characteristic broad emission lines and the optical to X-ray continuum obscured by a flattened torus of absorbing gas and dust (e.g. Mulchaey et al. 1994). This is the basis of the Unified Scheme for AGN (Antonucci 1993, Urry & Padovani 1995). NGC 4388 has been detected in X-rays for over 20 years (Table 1) and has always shown a column density, $N_H = 2-5\times 10^{23}\text{ cm}^{-2}$. The most common form of the Unified Scheme locates this absorption in a dusty torus at parsec distances from the central continuum (Krolik & Begelman 1988, Pier & Krolik 1992, 1993). However, Risaliti, Elvis & Nicastro (2002) found that 23/24 X-ray absorbed AGNs ($10^{22}\text{ cm}^{-2} < N_H < 3\times 10^{23}\text{ cm}^{-2}$) showed N_H variability by a factor 2-3. The best studied objects varied on the shortest accessible timescale of months, which is rather fast to be due to Keplerian motion at parsec radii and so raises questions about the nature of the obscuring torus.

Risaliti et al. suggested an alternative location in the cool outer parts of an accretion disk wind, echoing the model of Kartje, Königl & Elitzur (1999) who predicted just such a torus. This location predicts much faster N_H variability, down to a timescale of days. In a simple model of Poisson variations in the number of obscuring clouds, N_c , the amplitude of variability found by Risaliti et al., implies $N_c \sim 5-10$. In this case 0.1-1% of the time $N_c=0$ and, in the Unified scheme, the central type 1 nucleus would then be unveiled.

The RXTE (Swank et al. 1998) All Sky Monitor

(ASM, Remillard et al. 1997) is just sensitive enough to detect such low energy ‘unveiling events’. We thus began a Target of Opportunity (TOO) program with Rossi-XTE to obtain snapshot Proportional Counter Array (PCA, Swank et al. 1998) spectra of type 2 AGNs showing signs of a low energy detection in the RXTE ASM. Here we report the detection of a low N_H ‘unveiling event’ in NGC 4388.

2. OBSERVATIONS AND DATA REDUCTION

We monitored NGC 4388 with the RXTE ASM to search for detections in the soft 1.5 - 3 keV X-ray channel (‘a’). Normally NGC 4388 has a flux of $\sim 4\times 10^{-13}\text{ erg cm}^{-2}\text{ s}^{-1}$ in this band (Forman et al. 1979), while a detection requires a flux some 250 times larger ($\sim 1\times 10^{-10}\text{ erg cm}^{-2}\text{ s}^{-1}$). Simply removing the large absorbing N_H ($\sim 2-5\times 10^{23}\text{ cm}^{-2}$) would increase the observed flux to $\sim 4\times 10^{-11}\text{ erg cm}^{-2}\text{ s}^{-1}$, a factor of 100, so that only a modest additional factor 2-3 increase in the emitted continuum would be needed to put NGC 4388 over the threshold for ASM detection. By contrast, an increase in the emitted continuum flux by a factor >100 would be unprecedented among the well studied type 1 AGN, where factors of a few to ~ 10 variation are seen (Markowitz et al. 2003). Hence an ASM ‘a’ band detection is a good indicator of a low N_H event. A triggering event of this type occurred on 2003 May 9 (Fig. 1), shortly after another one (which is visible on the left of Fig. 1). One day after the ASM trigger NGC 4388 was observed twice with the RXTE PCA, for 1.9 ksec and 6.2 ksec, with a four hour gap between the two observations (Fig. 1).

We only consider data from PCU-2 for this analysis, as this is the best-calibrated proportional counter unit (PCU) in the RXTE/PCA⁵. Data reduction tools from LHEASOFT version 5.2⁶ were used to screen and prepare the event files and spectra. Data were taken in ‘Standard 2’ mode, which provides coverage of the full PCA bandpass (2–60 keV) every 16 seconds. Only

Electronic address: elvis@cfa.harvard.edu

¹ Harvard-Smithsonian CfA, 60 Garden St. Cambridge, MA 02138 USA

² INAF - Osservatorio di Arcetri, L.go E. Fermi 5, Firenze, Italy

³ NSF Astronomy and Astrophysics Postdoctoral Fellow

⁴ INAF - Osservatorio di Roma, Sede di Monteporzio Catone, Via di Frascati, 33, Monteporzio, Italy

⁵ URLs http://lheawww.gsfc.nasa.gov/users/keith/bkgd_status/status.html
<http://heasarc.gsfc.nasa.gov/listserv/grodis/msg00066.html>

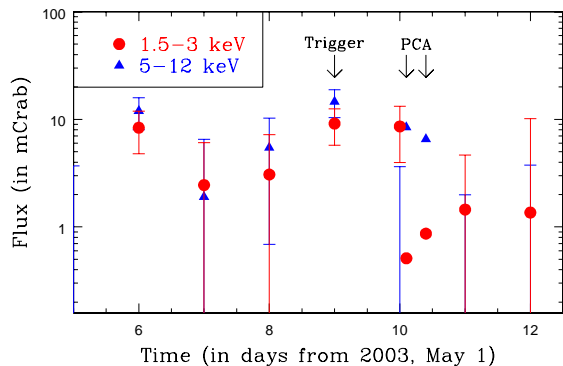


FIG. 1.— The RXTE All-Sky Monitor (ASM) light curve of NGC 4388 which triggered the pointed observations. The ‘a’ (1.5–3 keV) band fluxes are shown as circles and the ‘c’ (5–12 keV) band fluxes are shown as triangles. The triggering data points are marked. The two pointed PCA fluxes in the same bands are also shown. The error bars on the PCA measurements are smaller than the points.

data from the top Xe-filled gas layer in PCU-2 was used to make the source and background spectra, as this gas layer has the lowest background. The standard *RXTE* “good time interval” filtering was applied to the data. For the non-imaging PCA accurate background subtraction is crucial for faint sources like NGC 4388. The background spectra were made using the tool `pcabackest` using the latest ‘faint source’ background model (`pca_bkgd_cmfaint17_e5vv20031123.mdl`, updated by *RXTE* in November 2003). `pcabackest` calculates the predicted (dominant) particle background every 16 s, and so tracks the variation of the background around the orbit, thus taking into account the different backgrounds in these two short observations. Redistribution matrix files (`rmfs`) and ancillary response files (`arfs`) were made and combined into a single instrumental response file using `pcarsp`.

We added 0.6% systematic errors to our spectra using `grppha`, as we find that in many instances acceptable fits to the Crab can be obtained with 0.6% systematic errors. However, Poisson errors of 5% - 10% are dominant. The lowest channels in each of the PCUs routinely reveal strong deviations likely due to calibration uncertainties; in addition, the calibration of the PCUs is more uncertain above approximately 25 keV, and the spectra of faint sources like NGC 4388 become background-dominated in this regime. In fitting the spectra, then, we ignored energy range below 3 keV (channels 1-4) and above 20.0 keV. The PCA X-ray spectra are shown in Fig. 2a, where they are compared with a *Chandra* observation performed 14 months earlier. Fig. 2a shows that most of the variation is at low energies, <5 keV. In Fig. 2b we show the ratio between the two *RXTE* spectra, which indicates that the cut off in the spectra at low energies is due to a difference in N_H .

To fit the PCA spectra we used XSPEC v.11.3.7. A model comprising: a power-law of slope Γ , absorbed by a zero redshift N_H , with a superimposed emission line near the 6.4 keV Fe-K line energy, was fit to the two PCA data sets and gave good χ^2 (30/34 degrees of freedom for PCA-1 and 25/34 degrees of freedom for

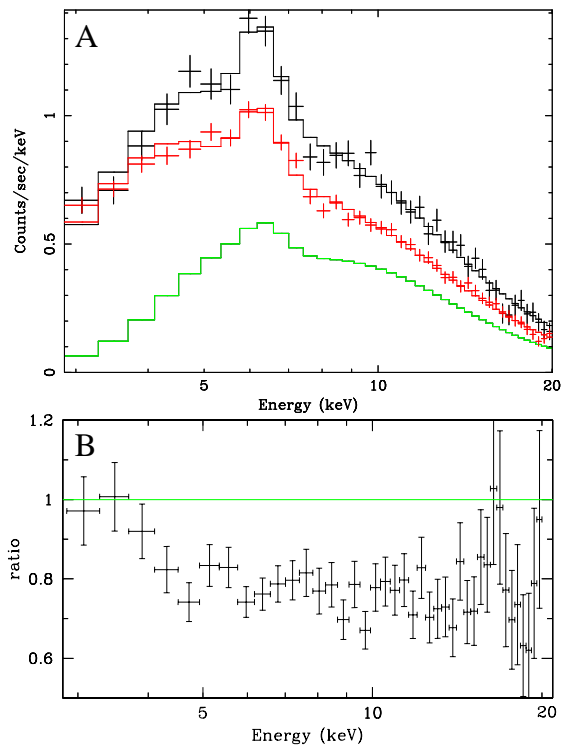


FIG. 2.— *Upper panel*: RXTE spectra of NGC 4388. For comparison, we also plot the best fit model of the *Chandra* observation performed one year earlier, convolved with the response and effective area of the PCA, and extrapolated from 10 keV to 20 keV for clarity. *Lower panel*: Ratio PCA-2/PCA-1, showing greater variability at low energies. No change in N_H would give a flat line.

PCA-2. The low redshift of NGC 4388 (2535 km s⁻¹ Huchra, Wyatt & Davis 1982) is indistinguishable from zero with the PCA. The Galactic N_H ($2.5 \times 10^{20} \text{ cm}^{-2}$, Murphy et al. 1996) is negligible for the PCA energy range. The total flux in the kiloparsec scale X-ray nebula around NGC 4388 (Iwasawa et al. 2003) is also negligible ($2.6 \times 10^{-13} \text{ erg cm}^{-2} \text{ s}^{-1}$). The results are given in Table 1, together with fits to the same model, with the same minimum energy, for two unpublished observations from XMM-Newton, and for six data sets from the literature. The measured N_H in the two PCA observations is $\sim 5 \times 10^{22} \text{ cm}^{-2}$ and $< 0.9 \times 10^{21} \text{ cm}^{-2}$, respectively (90% confidence). This rapid change between the two PCA observations in four hours is significant at the 3.2σ . I.e. there is a 0.14% chance that the N_H value is the same in the two PCA observations.

The PCA N_H values are one and two orders of magnitude respectively lower than in all previous X-ray observations of this source. In particular the PCA-1 N_H is 13σ smaller than that measured by XMM-Newton 5 months earlier (XMM-2, Table 1). [The change in N_H in the 5 months between XMM-1 and XMM-2 is significant at the 11σ level.] The contour plot of Fig. 3 shows that the dramatic reduction in N_H is not due to a degeneracy between Γ and N_H that is sometimes encountered in X-ray spectra. Γ is flat ($\Gamma=0.8-0.9$) in the PCA spectra compared both with most of the earlier observations and

⁶ URL <http://heasarc.gsfc.nasa.gov/docs/software/lheasoft/>

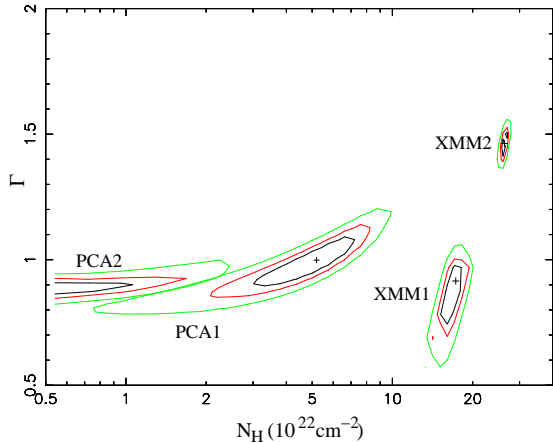


FIG. 3.— Photon index (Γ) vs. Column density (N_H) contour plots (68%, 90% and 99% confidence), derived here, for the two PCA observations of May 2003, and the two XMM-Newton observations of July 2002 and December 2002.

with unobscured type 1 AGNs ($\Gamma \sim 1.8$, Nandra et al. 1997, Reynolds 1997, Perola et al. 2002). The XMM-1 observation (Table 1) also gave a flat Γ , yet is heavily obscured, so a flat spectrum is not a property correlated with a low N_H . The small (~ 10 arcsecond) beam size of XMM-Newton (Jansen et al. 2001) effectively rules out the possibility that the flat PCA spectral slope is due to another source lying within the ~ 1 sq.degree PCA field of view. The high 2-10 keV flux in the BeppoSAX-1 observation demonstrates that a similarly high flux does not reduce the observed N_H . So we must be seeing bulk motion across our line of sight, as in Risaliti et al. (2002).

The N_H variation is robust against reasonable changes in the model: (1) Adding a reflection component (PEXRAV model, Magdziarz & Zdziarski 1995) does not alter Γ or N_H . Even leaving all the parameters free, the best fit is obtained with a covering factor ($R = \Omega/2\pi$) $R=0$. The 90% confidence upper limits are $R < 0.8$ for the first observation, and $R < 0.2$ for the second one. Fixing R to these upper limits we obtain column densities $N_{H1} \sim 2 \times 10^{21} \text{ cm}^{-2}$ and $N_{H2} \sim 8 \times 10^{22} \text{ cm}^{-2}$. (2) Adding a soft component, of course, does change the fit dramatically as this component affects only the lowest channels. For black body emission at typical soft excess temperatures of $kT \sim 0.3$ -1 keV the required 0.1-2 keV flux is 20 mCrab, or a luminosity of $5 \times 10^{42} \text{ erg s}^{-1}$. This luminosity causes no physical problems although a 10^4 s variation requires an optically thick source (Elvis et al. 1991 APJ 378, 537); a sphere of the implied area has a radius of only 10^{10} cm, 0.3 light-seconds. However such a large low energy flux is not suggested by the lowest energy PCA bins that were omitted from the fit.

The χ^2 test prefers an emission line consistent with the 6.4 keV Fe-K line, but broadened by $\sigma = 0.42_{-0.2}^{+0.14}$ keV (90% confidence), (i.e. FWHM = $2.38\sigma = 1.0$ keV, FWHM/E = 0.15c). A broad line would make an origin for the line in a parsec-scale torus unlikely, and would argue for wind or accretion disk origin. The XMM-2 observation however, using the higher spectral resolution CCD EPIC detectors, gives a lower gaussian σ (73 ± 20 eV), though the line may be complex. The PCA-2 measured equivalent width of the line, ~ 500 eV, is stronger than

normal for a type 1 Seyfert, but less strong than can be found in Compton thick AGN (Levenson et al. 2002). Again XMM-2 gives a more normal EW (~ 200 eV) for an AGN that is not Compton thick. The EW and σ of the PCA and XMM-1 are consistent but both disagree with the XMM-2 values.

3. DISCUSSION

We have found a factor 100 decrease in the column density toward the normally almost Compton thick ($\tau_{es} \sim 0.1$ -0.3) type 2 AGN NGC 4388. This decrease certainly occurred in less than the 0.4 years from the earlier XMM-Newton observation. The obscuring material in type 2 AGNs is thus in a highly dynamic state, and warrants intensive monitoring. A few strongly Compton thick AGN have become almost Compton thin on a timescale of 2.5 - 5.5 years (Matt, Guainazzi & Maiolino 2002), but not on shorter timescales, and still with residual column densities of $\sim 10^{23} \text{ cm}^{-2}$ even in the low absorption state, in 3 out of 4 cases. NGC 4388 is the only known case of an AGN in which a substantial X-ray opacity changes to an undetectable value ($\tau_{es} < 0.001$).

Moreover, it is likely that the decrease in obscuring column density coincided with the 2-day ‘flare’ seen in the RXTE ASM, so that the flare is primarily an ‘unveiling event’. Without X-ray spectra through the rise of the ASM flux, however, we cannot be certain. Between the two PCA observations we saw evidence, at 3.2σ , for a change of N_H in four hours.

The probable short timescale (either ~ 2 days or 4 hours) of the column density variations has strong implications for the location of the obscuring matter. Assuming that the absorption is due to clouds in Keplerian motion around the central source, and interpreting the 4 hour time lag between the two observations as the crossing time of a cloud implies a distance from the center $R < 10^4 \rho_{10}^2 t_4^2 R_S$, where ρ_{10} is the density in units of 10^{10} cm^{-3} , R_S is the Schwarzschild radius, and t_4 is the timescale in units of four hours (Risaliti et al. 2002). If NGC 4388 has an Eddington ratio of 0.1 then the black hole mass is $\sim 10^6 - 10^7 M_\odot$. Scaling from the K-band bulge magnitude gives a similar mass. This implies that the absorber is at a distance typical of the Broad Emission Line ‘clouds’ (BELRs), or smaller, and is of similar density. Only if a high density ($\rho > 10^{12} \text{ cm}^{-3}$) is assumed can a parsec distant absorber produce changes on the observed timescale (Fig. 4). A similar conclusion applies to the Seyfert 1.5 Galaxy NGC 4151, from the detection of a $\Delta(N_H) \sim 2 \times 10^{23}$ in a time interval of ~ 150 msec during a BeppoSAX observation (Puccetti et al. 2003).

This result is a challenge to the parsec scale usually attributed to the obscuring torus. For spherical isolated clouds, the high density implies small ($r_c \sim 10^{10}$ cm) cloud sizes: (1) The expansion time for a 100 K ($v_{sound} \sim 1 \text{ km s}^{-1}$) cloud from 10^{10} cm to 10^{11} cm is only 10^6 s, far shorter than the orbital time. But the large pressure needed to confine them ($p/k \sim 10^{14} \text{ K cm}^{-3}$) cannot be provided by self-gravity. (2) A hot confining medium would produce thermal emission much greater than the observed AGN bolometric luminosity (assuming a layer of 1 parsec thickness, $L_{gas} = 10^{48} T_7 n_7^2 \text{ erg s}^{-1}$, where T_7 and n_7 are the density and temperature in units of 10^7 K and 10^7 cm^{-3} , respectively, Rybicki & Lightman

Instrument	N_H^a	Γ	E_{Fe}^b	σ_{Fe}^c	EW_{Fe}^d	F^e	L^f	Obs. Date	Ref ^h
SL2-XRT	$2.1^{+2.8}_{-1.4}$	$1.9^{+0.9}_{-0.5}$	—	—	—	2.1	3.5	1985 Jul 29	1
ASCA-1	$3.15^{+1.1}_{-1.0}$	$1.32^{+0.77}_{-0.74}$	$6.49^{+0.09}_{-0.09}$	150^{+160}_{-130}	750^{+420}_{-300}	1.3	1.5	1994 Jul 04	2
ASCA-2	$3.34^{+1.0}_{-0.9}$	$1.47^{+0.57}_{-0.57}$	$6.47^{+0.07}_{-0.07}$	< 200	700^{+320}_{-250}	0.64	0.7	1995 Jun 21	2
BeppoSAX-1	$3.80^{+0.2}_{-0.4}$	$1.58^{+0.08}_{-0.22}$	$6.46^{+0.07}_{-0.10}$	< 230	233^{+115}_{-35}	2.5	3.5	1999 Jan 09	3
BeppoSAX-2	$4.80^{+1.8}_{-0.8}$	$1.47^{+0.04}_{-0.41}$	$6.38^{+0.05}_{-0.06}$	< 120	525^{+115}_{-112}	0.94	1.4	2000 Jan 03	3
Chandra	$3.50^{+0.4}_{-0.3}$	1.8^j	$6.36^{+0.02}_{-0.02}$	< 230	440^{+90}_{-90}	0.36	0.6	2001 Jun 08	4
Chandra-0	$2.50^{+0.2}_{-0.1}$	$1.25^{+0.14}_{-0.28}$	$6.36^{+0.03}_{-0.03}$	< 130	165^{+60}_{-60}	2.9	2.8	2002 Mar 05	5 ^k
XMM-1	$1.70^{+0.12}_{-0.15}$	$0.91^{+0.10}_{-0.37}$	$6.41^{+0.02}_{-0.02}$	< 77	503^{+70}_{-60}	0.77	0.7	2002 Jul 07	5
XMM-2	$2.61^{+0.06}_{-0.06}$	$1.46^{+0.04}_{-0.05}$	$6.44^{+0.02}_{-0.02}$	73^{+20}_{-20}	204^{+24}_{-26}	2.0	2.2	2002 Dec 12	5
RXTE/PCA-1	$0.52^{+0.25}_{-0.24}$	$0.99^{+0.11}_{-0.11}$	$6.34^{+0.11}_{-0.11}$	< 380	503^{+138}_{-100}	7.2	4.0	2003 May 10 ^g	5
RXTE/PCA-2	< 0.09	$0.86^{+0.07}_{-0.03}$	$6.32^{+0.10}_{-0.09}$	390^{+160}_{-190}	570^{+114}_{-100}	6.1	2.9	2003 May 10 ^g	5

TABLE 1

^a ABSORBING COLUMN DENSITY, N_H , IN UNITS OF 10^{23} cm^{-2} . ^b PEAK ENERGY OF THE IRON $K\alpha$ LINE, KEV. ^c WIDTH OF THE IRON LINE, IN EV. ^d EQUIVALENT WIDTH OF THE IRON LINE, IN EV. ^e OBSERVED 2-10 KEV FLUX, IN UNITS OF 10^{-11} ERG s^{-1} CM^{-2} . ^f INTRINSIC 2-10 KEV LUMINOSITY, IN UNITS OF 10^{42} ERG s^{-1} CM^{-2} (ASSUMING A VIRGO CLUSTER LOCATION AT 20 MPC, TAMMANN ET AL. 1999). ^g XTE OBSERVATIONS 4 HOURS APART. ^h REFERENCES: 1: HANSON ET AL. 1990; 2: FORSTER, LEIGHLY & KAY 1999; 3: RISALITI 2002; 4: IWASAWA ET AL. 2003; 5: THIS WORK. ^j FIXED. ^k 0-ORDER SPECTRUM FROM HETGS OBSERVATION (OBSID=2983).

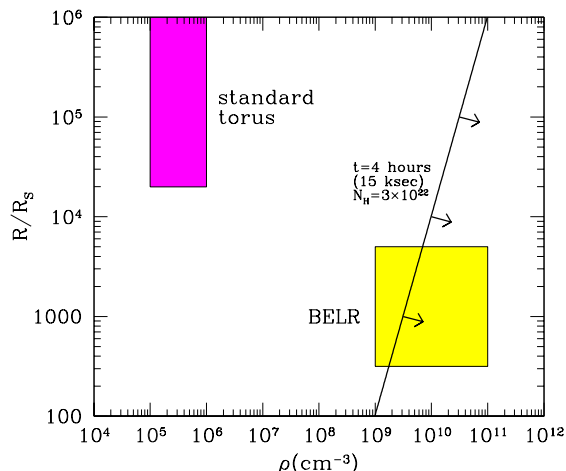


FIG. 4.— Distance (R/R_s) vs. density (ρ) plot for AGN X-ray absorbers. The “standard torus” of the unified model has a density $n < 10^6$ cm^{-3} . Variability of the absorber in 4 hours or less rules (solid diagonal line) out an absorber with such properties, and is more compatible with the standard parameters of the Broad Emission Line Clouds (BELR).

1979). (3) The N_H through a confining medium would be $10^{25.5} n_7 \times d_{pc} \text{ cm}^{-2} = 10\tau_{es}$. So all continuum variations shorter than a few years would be smeared out by Thomson scattering, contrary to observations (Table.1). (4) Individual clouds would cover only a small fraction, $\sim 10^{-6}$, of the X-ray emitting source, whose dimensions are $> 10^{13}$ cm for a black hole of mass $> 10^7 M_\odot$. If hundreds of clouds are needed to cover the X-ray source, no N_H variation by more than a few percent can be observed with significant probability.

To produce large variations in N_H compatible with $< N_c > \sim 5-10$ needs clouds of a diameter within a factor of a few of the continuum source size. This implies a density of $\sim 10^9 \text{ cm}^{-3}$. This is just compatible with a radius $R \sim \text{few} 100 R_s$ given a 4 hour variation (Fig.4). If the absorbers are part of a wind crossing our line of sight (Elvis 2000) then sheet-like structures (Arav et al. 1998) become plausible, and this allows larger radii.

The great majority (>99%) of the obscuring *gas* in NGC 4388 occurs at small radii, and the most likely scenario is that Broad Emission Line clouds are drifting across our line of sight in NGC 4388 leading to large changes in N_H . Similar behavior has been seen in some type 1 AGN, involving an $N_H \sim 10^{23} \text{ cm}^{-2}$ over $\sim 100^d$ at the radius of the BELR (Lamer, Uttley & Miller 2003). Since we have no simultaneous optical spectra we do not know whether the bulk of the dust, which absorbs the optical and UV photons, lies on the same small scale. The closest dust could be to the continuum is the sublimation radius (Barvainis 1987) which, in NGC 4388 at $\sim 10^{42}$ erg s^{-1} (2-10 keV), is $\sim 7 \times 10^{16}$ cm (0.02 pc), or $2 \times 10^4 r_s (M_7)$ (fig.4). The dust:gas ratio in AGN is typically a factor 10 below the Milky Way value (Maccacaro et al. 1982, Maiolino et al. 2001), so that a separate dusty absorber is allowed. Unveiling events in type 2 AGN, such as the one reported here for NGC 4388, put strong constraints on Unified Models for AGN, and seem to point to a different view of the obscuring torus.

This paper used results provided by the ASM/RXTE teams at MIT and at the RXTE SOF and GOF at NASA’s GSFC. JMM acknowledges the NSF. This work was partially supported by Chandra grant GO2-3122A.

REFERENCES

- Antonucci, R. 1993, ARA&A, 31, 473
 Arav, N., Barlow, T. A., Laor, A., Sargent, W. L. W., & Blandford, R. D. 1998, MNRAS, 297, 990
 Barvainis R., 1987, ApJ, 412, 513.
 Elvis M., 2000, ApJ, 545, 63.
 Forster, K., Leighly, K. M., & Kay, L. E. 1999, ApJ, 523, 521
 Hanson, C. G., Skinner, G. K., Eyles, C. J., & Willmore, A. P. 1990, MNRAS, 242, 262
 Huchra, J. P., Wyatt, W. F., & Davis, M. 1982, AJ, 87, 1628
 Iwasawa K., Wilson A.S., Fabian A.C. & Young A.J., 2003, MNRAS, 345, 369.
 Jansen, F. et al. 2001, A&A, 365, L1
 Kartje, J. F., Königl, A., & Elitzur, M. 1999, ApJ, 513, 180
 Khachikian, E. Y. & Weedman, D. W. 1974, ApJ, 192, 581
 Krolik, J. H. & Begelman, M. C. 1988, ApJ, 329, 702
 Lamer G., Uttley P. & McHardy I.M., 2003, MNRAS, 342, L41.
 Levenson N., et al. 2002, ApJ, 573, L81.
 Magdziarz P. & Zdziarski A.A., 1995, MNRAS, 273, 837

- Markowitz A., Edelson R., Vaughan S., Uttley P., George I.M., Griffiths R.E., Kaspi S., Lawrence A., McHardy I., Nandra K., Pounds K.A., Reeves J., Schurch N., Warwick, R.
- Matt G., Guainazzi M. & Maiolino R., 2002, MNRAS 342, 422
- Murphy E.M., Lockman F.J., Laor A. & Elvis M., 1996, ApJS, 105, 369.
- Nandra, K., George, I. M., Mushotzky, R. F., Turner, T. J., & Yaqoob, T. 1997, ApJ, 476, 70
- Perola, G. C., Matt, G., Cappi, M., Fiore, F., Guainazzi, M., Maraschi, L., Petrucci, P. O., & Piro, L. 2002, A&A, 389, 802
- Pier, E. A. & Krolik, J. H. 1992, ApJ, 399, L23
- Pier, E. A. & Krolik, J. H. 1993, ApJ, 418, 673
- Puccetti, S., Risaliti, G., Fiore, F., Elvis, M., Nicastro, F., Perola, G.C., Capalbi, M. 2003, Proc. of the BeppoSAX Symposium, The Restless High-Energy Universe, E.P.J. van den Heuvel, J.J.M. in 't Zand, and R.A.M.J. Wijers (Eds), astro-ph/0311446
- Remillard, R. A. & Levine, A. M. 1997, All-Sky X-Ray Observations in the Next Decade, 29
- Reynolds, C. S. 1997, MNRAS, 286, 513
- Risaliti, G. 2002, A&A, 386, 379
- Risaliti, G., Elvis, M., & Nicastro, F. 2002, ApJ, 571, 234
- Rybicki G. & Lightman A.P., 1979, *Radiative Processes in Astrophysics* [Wiley, New York].
- Tammann, G. A., Sandage, A., & Reindl, B. 1999, proceedings of the 19th Texas Symposium on Relativistic Astrophysics and Cosmology, held in Paris, France, Dec. 14-18, 1998. Eds.: J. Paul, T. Montmerle, and E. Aubourg (CEA Saclay), astro-ph/9904360
- Swank, J. H. 1998, The Active X-ray Sky: Results from BeppoSAX and RXTE, 12
- Urry, C. M. & Padovani, P. 1995, PASP, 107, 803